^{1}H NMR Structure and Biological Studies of the His^{23} → Cys Mutant Nucleocapsid Protein of HIV-1 Indicate That the Conformation of the First Zinc Finger Is Critical for Virus Infectivity†

H. Déméné,‡ C. Z. Dong,‡ M. Ottmann,§ M. C. Rouyez,‖ N. Jullian,‡ N. Morellet,‡ Y. Mely,⊥ J. L. Darlix,§ M. C. Fournié-Zaluski,‡ S. Saragosti,‖ and B. P. Roques*,‡

Département de Pharmacochimie Moléculaire et Structurale, U266 INSERM-URA D1500 CNRS, Faculté de Pharmacie, Université René Descartes, 4, Avenue de l'Observatoire, 75270 Paris Cedex 06, France, LaboRétro, U412 INSERM, ENS de Lyon, 46, Allée d'Italie, 69634 Lyon Cedex 07, France, Département d'Immunologie et Oncologie des Maladies Rétrovirales, U152 INSERM, CHU Cochin-Port-Royal, 27, Rue du Faubourg Saint-Jacques, 75674 Paris Cedex 14, France, and Laboratoire de Biophysique, Faculté de Pharmacie de Strasbourg, 74, Route du Rhin, B.P. 24, 67401 Illkrich Cedex, France

Received April 18, 1994; Revised Manuscript Received July 14, 1994®

ABSTRACT: The nucleocapsid protein NCp7 of human immunodeficiency virus type 1 (HIV-1), which has key functions in the virus life cycle, possesses two zinc fingers of the $CX_2CX_4HX_4C$ type characterized by three successive loops containing a tetrahedrally coordinated zinc atom. The replacement of any cysteine by a serine in either finger has been shown to result in the production of noninfectious viruses, probably by impairing the biological functions of NCp7. In order to more precisely elucidate the structural role of the zinc finger motif, His^{23} was replaced by Cys in the proximal finger of the peptide (13–64)NCp7 which retains NCp7 activities *in vitro*. The peptide Cys^{23}(13–64)NCp7 was synthesized by solid phase and studied by 2D ^{1}H NMR and molecular modeling. The His to Cys modification causes important structural modifications of the N-terminal zinc finger which impair the spatial proximity of the two zinc fingers as shown by the disappearance of several interresidue NOEs. The side chains of Val^{13}, Lys^{14}, Phe^{16}, Thr^{24}, Ala^{25}, Trp^{37}, Gln^{45}, and Met^{46}, which are thought to be involved in nucleic acid recognition, are no longer found clustered in the Cys^{23}(13–64)NCp7 mutant as they are in the wild-type NCp7 structure. *In vitro*, Cys^{23}(13–64)NCp7 is unable to tightly interact with the viral RNA or replication primer tRNA^{Lys,3}. The Cys^{23}(NCp7) mutation was introduced into an infectious HIV-1 molecular clone, and virions produced upon DNA transfection into cells were analyzed for their viral protein and RNA compositions as well as for their infectivity. Results show that, while the Cys^{23}(NCp7) mutation does not impair virion production, viruses contain a low amount of degraded viral RNA and are not infectious. These findings suggest that a *bona fide* conformation of the HIV-1 NCp7 is critical for the packaging of viral RNA, its stability in virions, and virus infectivity.

The nucleocapsid protein NCp7 of human immunodeficiency virus type I (HIV-1),[1] which is part of the C-terminal domain of the polyprotein precursor Pr55gag, is a small basic peptide (72 amino acids) tightly associated with the dimeric RNA genome in the core of the viral particle (Darlix *et al.*, 1990). At this level, nonspecific interactions of NCp7 molecules with the genomic RNA could ensure its protection from nucleases (Aronoff *et al.*, 1993). NCp7 contains two motifs of the type $CX_2CX_4HX_4C$ also found in the nucleocapsid proteins of other retroviruses (Henderson *et al.*, 1981; Berg *et al.*, 1986). The two CCHC domains of NCp7 bind zinc with high affinity ($K_A \sim 10^{13}$ M^{-1}) (Mély *et al.*, 1991), and the metal ions were shown by various methods, including EXAF studies, to be tetracoordinated to the three cysteines and the histidine (South *et al.*, 1989, 1991; Summers *et al.*, 1990; Fitzgerald & Coleman, 1991; Omichinski *et al.*, 1991; Morellet *et al.*, 1992; Summers *et al.*, 1992) as initially proposed by Berg (1986). NMR studies have shown that the typical folding around the metal observed in isolated zinc fingers is conserved in the three-dimensional solution structure of HIV-1 NCp7 (Summers *et al.*, 1992; Omichinski *et al.*, 1991; Morellet *et al.*, 1992) and nucleocapsid protein NCp10 of murine leukemia virus (MuLV) (Déméné *et al.*, 1994). Moreover, a temperature-dependent conformation of NCp7, characterized by a proximity between the two zinc fingers, was proposed to account for long-range NOEs between amino acids present in the zinc fingers (Morellet *et al.*, 1992, 1994).

In vitro, NCp7 was found to promote the annealing of replication primer tRNA^{Lys,3} onto the genomic RNA at the initiation site for reverse transcription (PBS) (Barat *et al.*, 1989; de Rocquigny *et al.*, 1992) and to stimulate minus-strand DNA synthesis (Darlix *et al.*, 1990). Also, NCp7 was shown to activate viral RNA dimerization *in vitro*, a process most probably related to genomic RNA packaging in virions (Darlix *et al.*, 1990). *In vivo*, NCp7, either as the free protein or as part of the Pr55gag precursor, was reported to direct genomic RNA packaging (Gorelick *et al.*, 1988; Göttlinger *et al.*, 1989; Aldovini & Young, 1990; Berkowitz *et al.*, 1993).

The CCHC zinc fingers of retroviral NC proteins were found to be of importance for genomic RNA packaging since point mutations of the conserved cysteine and histidine residues

† This work was supported by a grant from the Agence Nationale de Recherche sur le SIDA (ANRS).

* To whom correspondence should be addressed [telephone (33) 1-43.25.50.45; FAX (33) 1-43.26.69.18].

‡ Faculté de Pharmacie, Université René Descartes.

§ ENS de Lyon.

‖ CHU Cochin-Port-Royal.

⊥ Faculté de Pharmacie de Strasbourg.

® Abstract published in *Advance ACS Abstracts,* September 1, 1994.

[1] Abbreviations: DLS, dimer linkage structure; HIV-1, human immunodeficiency virus type 1; PBS, primer binding site; 2D ^{1}H NMR, two-dimensional nuclear magnetic resonance.

0006-2960/94/0433-11707$04.50/0

in HIV-1 NCp7 (Gorelick *et al.*, 1990; Dorfman *et al.*, 1993) as well as in MuLV NCp10 (Gorelick *et al.*, 1988; Méric & Goff, 1989) and RSV NCp12 (Méric *et al.*, 1988; Dupraz *et al.*, 1990) resulted in a drastic reduction of packaged genomic RNA dimer in virions. However, since all of the mutations studied, like substitution of Ser for Cys or Ala for His, prevented the formation of the highly stable tetrahedral zinc coordination (Green & Berg, 1990; Mély *et al.*, 1991), the role of the CCHC zinc finger and the extent of its specificity are poorly understood.

In the present study, the role of the spatial arrangement of the CCHC zinc finger in the biological functions of HIV-1 NCp7 *in vitro* and *in vivo* was investigated by substituting Cys for His^{23} in the first finger motif of NCp7. This change was expected to preserve the strong affinity of the mutated finger for the zinc atom since several proteins known to interact with nucleic acids contain zinc binding domains of the CCCC form [reviewed in Berg *et al.* (1990) and Angrand (1993)]. Accordingly, we have shown in a preliminary report that replacement of His^{23} by Cys in the isolated N-terminal finger of NCp7 led to a folded structure in which the four cysteines coordinated the zinc atom (Jullian *et al.*, 1993). Since (13–64)NCp7 was found to be as active as NCp7 in assays performed *in vitro* (de Rocquigny *et al.*, 1992), the Cys^{23}-(13–64)NCp7 mutant was synthesized by solid phase and its solution structure determined by 2D ^1H NMR spectroscopy and molecular modeling. The mutant peptide is characterized by a folding of the N-terminal CCCC box similar to that of the mutated zinc finger alone (Jullian *et al.*, 1993) but clearly different from the CCHC domains found in the native (13–64)NCp7. In particular, the disappearance of numerous long-range NOEs observed in the wild-type protein suggests the occurrence of a structural modification in Cys^{23}(13–64)NCp7. Although the distal zinc fingers were shown to adopt the same conformation in both (13–64)NCp7 and Cys^{23}(13–64)NCp7 proteins, none of the ^1H NMR derived structures of Cys^{23}-(13–64)NCp7 were similar to that of the wild-type protein. *In vitro*, Cys^{23}(13–64)NCp7 was found to be poorly active. This is probably due to an extensive inhibition of NC protein–RNA interactions caused by the His^{23} to Cys mutation. To investigate the effects of this Cys^{23} mutation *in vivo*, an infectious HIV-1 molecular clone with the Cys^{23}-NC mutation was transfected into cells. HIV-1 mutant virions were produced but were shown to be noninfectious.

EXPERIMENTAL PROCEDURES

Chemicals. In order to carry out NMR experiments, large quantities of (13–64)NCp7 and of mutant Cys^{23}(13–64)NCp7 were synthesized using the stepwise solid-phase method and Fmoc amino acids on an reprogrammed automatic Applied Biosystems 431A synthesizer as previously described (de Rocquigny *et al.*, 1991).

NMR Experiments. NMR samples were prepared by dissolving 16 mg of (13–64)NCp7 or Cys^{23}(13–64)NCp7 in 0.5 mL of 90% H_2O/10% D_2O in the presence of 2.1 equiv of zinc chloride. The pH was adjusted to the desired value with small aliquots of 1 M NaOD or 1 M DCl. NMR data were collected on a Bruker AMX 600 spectrometer operating at 600 MHz for protons, with the carrier frequency set to the resonance of water. ^1H NMR chemical shifts were referenced to internal H_2O. 2D NMR data were collected without sample spinning and at 20 °C except where noted. Irradiation of the water resonance was performed during relaxation delay and during the mixing time for NOESY experiments. Pulse sequences are described below. For most experiments, 512 t_1 values were usually acquired with either 64 or 128 scans per t_1 increment. 2D NMR spectra were recorded in the phase-sensitive mode using the time-proportional phase incrementation method (Marion & Wüthrich, 1983). The spectral width was about 12 ppm in both dimensions. Most of the 2D NMR data were then processed with zero filling to a final spectrum of 2048 × 1024 points. All free induction decays were multiplied by shifted sine-bell windows in both dimensions. Additional base-line corrections were performed using polynomial functions of standard Bruker software installed on a Bruker X32 computer.

Phase-sensitive Clean TOCSY spectra (Braunschweiler & Ernst, 1983; Davis & Bax, 1985; Griesinger *et al.*, 1988) were obtained for aqueous samples with a total mixing time of 55 and 87 ms. The extended MLEV cycle was preceded and followed by a 2.5-ms trim pulse to defocus magnetization not parallel to the spin lock axis. A DQF COSY experiment (Rance *et al.*, 1982) was also performed. NOESY spectra (Jeener *et al.*, 1979; Macura *et al.*, 1981) were recorded with mixing times of 100 and 200 ms at 20 °C and 200 ms at 30 °C. No zero-quantum suppression technique was applied. The relaxation delay was 2 s.

NMR-Derived Constraints. NOEs observed in the 100-ms NOESY spectra were used as modeling constraints. Additional NOEs observed in the 200-ms NOESY experiment were used as modeling constraints only when all possible spin diffusion pathways could be discarded (Kochoyan *et al.*, 1991). The classification of NOEs as strong, medium, and weak was made on the basis of the their relative amplitude to cysteine geminal proton NOEs used as the internal standard.

Structure Calculations. A total of 636 distance constraints derived from NMR experiments were classified into three categories: 2.0–2.5, 2.0–3.5, and 2.0–4.5 Å corresponding to strong, medium, and weak NOEs, respectively. The interactions between the Cys and His residues and the zinc atoms were defined on the basis of cadmium-complexed metallothionein (Arseniev *et al.*, 1988), leading to additional modeling constraints. As previously described (Morellet *et al.*, 1992), the zinc atoms were introduced as pseudoatoms QZn linked to the sulfur atoms of the relevant Cys residues with a bond length of 2.3 Å. In the second zinc finger, the distance between the QZn and the Nε2 atoms of His^{44} was constrained to 2.0 Å. In each zinc finger domain, the distance between the QZn atoms was imposed to be less than 0.1 Å, thus mimicking the unique zinc ion (Arseniev *et al.*, 1988).

Introduction of classified NOEs in the DIANA distance geometry package (Güntert *et al.*, 1991a), with standard parameters as described by Güntert *et al.* (1991b), produced a preliminary group of structures which was used to refine the set of NOE distance constraints. The 20 best structures based on an arbitrary final error function cutoff were then refined by energy minimization using the AMBER package (Pearlman *et al.*, 1991) with a conjugated gradient method. A zinc force field derived from *ab initio* calculations was parameterized in the AMBER framework in order to take into account metal–protein interactions (Jacob, 1990). Moreover, a dielectric constant of 80 was used to minimize ion pair interactions overestimated in *in vacuo* simulations. Computer graphic representations were obtained using the INSIGHT molecular modeling package (BIOSYM Technologies Inc., San Diego, CA) on a personal IRIS 4D35 workstation (Silicon Graphics Inc.). All structural calculations were performed on a RISC System/6000–550 workstation.

Fluorescence Parameters. Fluorescence experiments were performed in 50 mM Hepes (pH 7.5) and 0.1 M KCl with

Cys^{23}(13–64)NCp7 or (13–64)NCp7 (6×10^{-6} M). Fluorescence spectra were obtained with a SLM 48000 spectrofluorometer at 20 ± 0.5 °C. The excitation wavelength was set at 295 nm for selective excitation of Trp residues. Quantum yields were determined using L-Trp in water ($\Phi = 0.14$) as a reference (Eisinger & Navon, 1969). Zinc titration experiments were performed by following the fluorescence intensity changes at the maximum emission wavelength (351 nm) as described (Mély *et al.*, 1991).

Analysis of Nucleocapsid Protein NCp7 Activity in Vitro. Preparation of HIV-1 RNA (positions 1–415) unlabeled or ^{32}P-labeled was carried out as previously described (Darlix *et al.*, 1990). Replication primer tRNA^{Lys,3} labeled with ^{32}P was synthesized *in vitro* and subsequently purified by polyacrylamide gel electrophoresis exactly as reported before (Barat *et al.*, 1991). Gel retardation assays were performed under conditions already described (Darlix *et al.*, 1990; Bieth *et al.*, 1990). Assays were in 10 μL containing 25 mM Tris-HCl (pH 7.5), 60 mM NaCl, 0.2 mM $MgCl_2$, 5 mM DTT, 200 ng of ^{32}P-HIV-1 RNA, and 0.1–10 μM NCp7, (13–64)-NCp7, or Cys^{23}(13–64)NCp7. After 5 min at 37 °C, SDS (0.1% final), glycerol (10% final), and bromophenol blue (0.01% final) were added and the samples analyzed by 5% polyacrylamide gel electrophoresis (PAGE) in 50 mM Tris–borate (pH 8.3) at 20 °C. Autoradiography of the wet gel was for 3–6 h at 4 °C.

Ultraviolet light (UV 252 nm) irradiation of the NC protein–RNA complexes was performed exactly as described in Darlix *et al.* (1990) and de Rocquigny *et al.* (1993). NC protein–primer ^{32}P-tRNA^{Lys,3} complexes were analyzed by 10% PAGE in the presence of 0.2% SDS. NC protein–^{32}P-RNA complexes were digested for 30 min at 20 °C with 5 units of T_1 RNase, then incubated in 5 mM EDTA and 1% SDS for 2 min at 80 °C, and analyzed by 15% PAGE/0.2% SDS.

Annealing of replication primer ^{32}P-tRNA^{Lys,3} to the primer binding site (PBS) of the viral RNA was conducted exactly as described before (Barat *et al.*, 1989; de Rocquigny *et al.*, 1992).

HIV-1 DNA Mutagenesis and Construction. Two infectious HIV-1 molecular clones [HIV-1 LAI, a gift of Peden *et al.* (1991), and HIV-1 pNL4.3 (Adachi *et al.*, 1986)] were used in these assays, and results were identical (see below). The 1299-bp *Bss-Apa*I fragment (positions 257–1556) of HIV-1 LAI was cloned into pBluescript KS (Stratagene, La Jolla, CA). Subsequently, the His codon CAC was mutated to give the Cys codon TGT. Site-directed mutagenesis of the *Sph*I–*Eco*RI fragment of HIV-1 pNL4.3 in M13mp19 was carried out according to a standard protocol (Kunkel, 1985). The mutated DNA fragments were verified by sequencing and reinserted into HIV-1 LAI or pNL4.3.

DNA Transfection and HIV-1 Virion Analysis. Proviral DNA transfection of Cos7 cells was performed by the calcium phosphate mediated procedure (Chen & Okayama, 1987) using 5–10 μg of DNA. At day 3, supernatant from transfected cells was harvested, clarified by low-speed centrifugation (3000 rpm, 15 min), and assayed for viral CAp24 core antigen by ELISA (kindly provided by V. Cheney and B. Mandrand, Biomérieux) and reverse transcriptase (RT) activity using a modified protocol initially described by Goff *et al.* (1981). Virus titer was assessed by infecting 1×10^6 human SupT1 cells (Smith *et al.*, 1984) with 1 mL of clarified supernatant and monitoring virion-associated RT activity 4–20 days after infection [see also Morellet *et al.* (1994)]. Remaining supernatant containing virions was ultracentrifuged through a 20% sucrose cushion in TNE [25 mM Tris-HCl (pH 7.5), 50 mM NaCl, 1 mM EDTA]. Virion pellets were dissolved in TNE/1% SDS and the proteins fractioned through a 5–15% gradient polyacrylamide gel in Tricine buffer (Schägger & von Jagow, 1987) and subsequently electrotransferred onto a nitrocellulose membrane. Immunoblot analysis was performed using a chemoluminescent procedure (ECL, Amersham) according to the manufacturer's instructions with CAp24/Map17, RTp66/p51 antisera, and NCp7 monoclonal antibodies (kindly provided by V. Tanchou and R. Bénarous).

Viral RNA from virus particles was isolated from concentrated transfected cell supernatant after proteinase K treatment by phenol/chloroform extraction followed by ethanol precipitation. Samples were adjusted for equal amounts of Cap24 before electrophoresis of viral RNA in a 0.7% agarose/MOPS/formaldehyde gel and then electroblotted onto a nylon membrane (Hybond N, Amersham). HIV-1 genomic RNA was probed with a nick-translated, ^{32}P-labeled 5.3-kb *Sac*I–*Sal*I fragment of the pNL4.3 plasmid corresponding to the gag and pol sequences to probe the unspliced viral RNA.

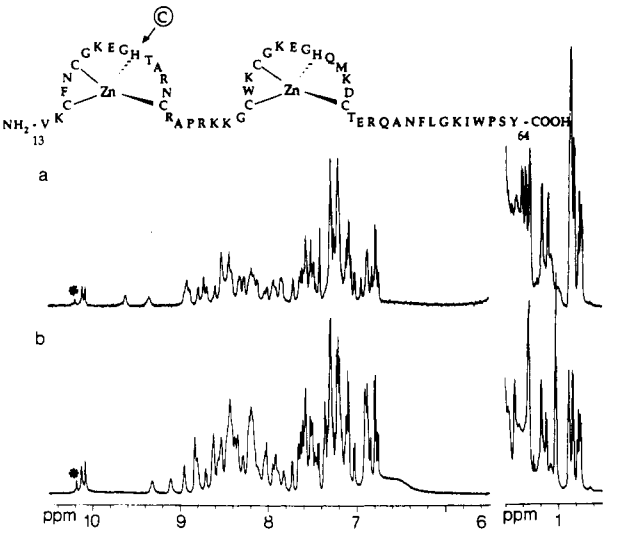

FIGURE 1: Scheme of the (13–64)NCp7 sequence showing the site of the His^{23} → Cys mutation (top). Selected regions of the 600-MHz ^{1}H NMR spectra of (a) (13–64)NCp7 and (b) Cys^{23}(13–64)NCp7. In each spectrum, the small peak around 10.2 ppm (*) corresponds to the minor population associated with the Pro^{62} cis conformation.

RESULTS

NMR Experiments. In the presence of 2 equiv of zinc, the spectrum of (13–64)NCp7 and Cys^{23}(13–64)NCp7 at pH 6.5 exhibited NH resonances scattered over a wide range of frequencies, demonstrating that these peptides interacted with the metal and that the binding of zinc induced a folding of the finger domains into well-defined conformations (Figure 1a,b).

NMR Assignment of Cys^{23}(13–64)NCp7. Sequence-specific assignment of Cys^{23}(13–64)NCp7 protons was obtained by first identifying amino acid spin systems using direct and relayed through-bond connectivities, followed by the sequential assignment of resonances by means of short (<5 Å) through-space connectivities (Wüthrich, 1986). The first step was done using DQF spectra as shown in Figure 2 for the fingerprint region of Cys^{23}(13–64)NCp7. The sequential assignment was carried out by identifying short-range NOEs involving NH, αH, and βH protons in the NOESY spectra. Ambiguities could generally be resolved using NOESY spectra recorded at 20 and 30 °C. For this 52 amino acid residue peptide, 49 $d_{\alpha N}$ NOEs were expected. Of these, only 37 were

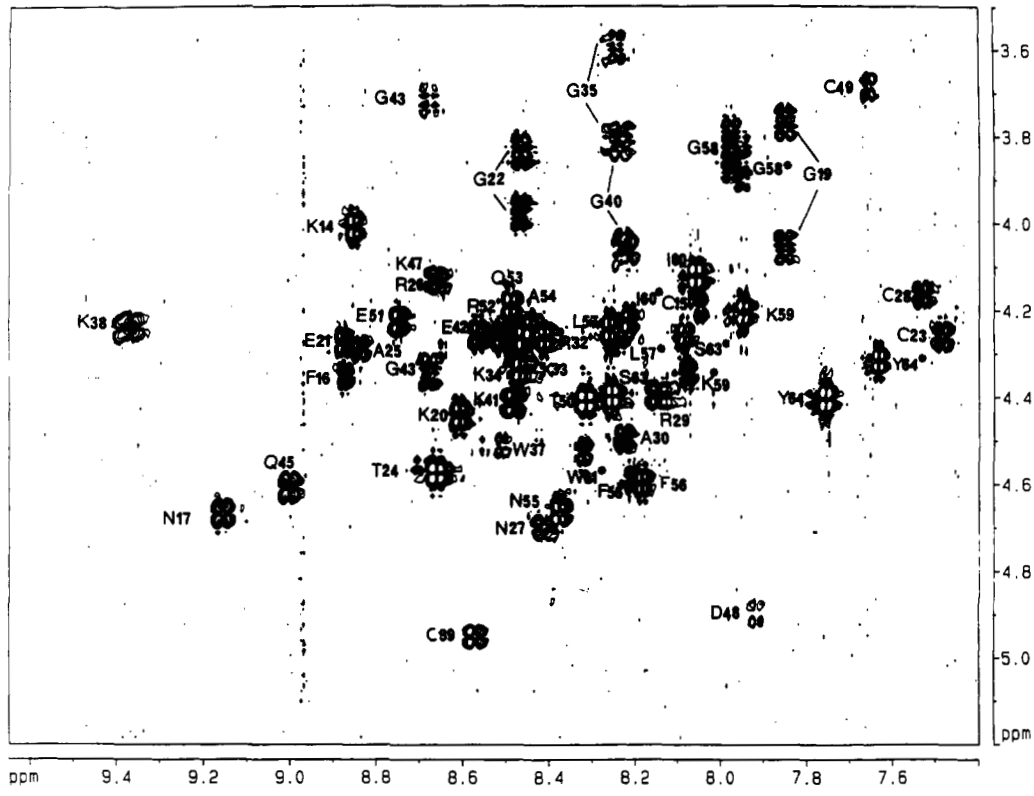

FIGURE 2: Fingerprint region of the DQF COSY spectrum recorded for mutant Cys[23](13–64)NCp7 in H_2O at pH 6.5 and 20 °C. Residues labeled with an asterisk correspond to the minor population associated with the Pro[62] cis conformation.

observed. The remaining connectivities were not observed due either to a partial saturation of the corresponding αH resonances or to resonance overlapping. This problem was overcome by using NH/NH and $NH_{i+1}/H\beta_i$ connectivities. Prolines were sequentially assigned from $H\alpha_i/H\delta_{i+1}$ connectivities. As reported for native NCp7 (Morellet *et al.*, 1992), evidence of cis–trans equilibrium was found for Pro[62]. Under the present experimental conditions, all amino acid residues within the sequence 56–64 of Cys[23](13–64)NCp7 exhibited double resonances for their backbone and aliphatic protons (residues labeled with an asterisk in Figure 2). As for NCp7, the series of signals corresponding to Pro[62] in the cis conformation formed the minor population. Cys[23](13–64)-NCp7 ^{1}H NMR chemical shifts are listed in Table 1 (supplementary material) and were compared with those of the native (13–64)NCp7 peptide. The chemical shift differences between the backbone protons of the Cys[23](13–30)-NCp7 N-terminal zinc finger (Jullian *et al.*, 1993) and the corresponding protons in Cys[23](13–64)NCp7 were very weak (data not shown), suggesting that the addition of the 30–64 C-terminal region did not significantly modify the spatial arrangement of the four cysteine box. This is in contrast to results obtained for the native NCp7 in which a similar extension produced changes in the chemical shifts of aromatic residues in both zinc fingers (Morellet *et al.*, 1992). Inspection of chemical shift differences between native (13–64)NCp7 and mutant Cys[23](13–64)NCp7 (Table 1, supplementary material) reveals that the linker region RAPRRKG was also affected by the mutation His[23] to Cys[23]. Significant differences in chemical shifts of the Pro[31]–Lys[34] segment indicate that the protons of this region were in different chemical environments in the two peptides. In contrast, the positions of NMR resonances corresponding to protons of the distal zinc finger are identical in (13–64)NCp7 and its Cys[23] mutant (Table 1, supplementary material).

NMR Parameters of the Zinc Finger and Linker Domains of Cys[23](13–64)NCp7. Comparison with (13–64)NCp7. (A) Proximal 13–30 Zinc Finger. As already observed with the mutant Cys[23](13–30)NCp7 finger studied alone (Jullian *et al.*, 1993), two segments (Phe[16]–Lys[20] and Ala[25]–Ala[30]) of intense NH/NH connectivities were seen in the proximal finger domain of Cys[23](13–64)NCp7. The NMR constraints accounting for elements of secondary structure in Cys[23](13–64)NCp7 and in the native peptide are available in supplementary material (Figure 1). Furthermore, a series of long-range NOEs was observed in the NOESY spectra of Cys[23](13–64)NCp7 but not in the native protein (Figure 3): NH(Cys[15])/Hα(Glu[21]), Hα(Cys[28])/Hβ(Asn[17]), Hα(Ala[25])/Hβ(Asn[17]), Hα(Gly[19])/Hβ(Lys[14]), Hβ(Arg[29])/Hβ(Ala[25]), Hα(Lys[14])/Hβ(Cys[23]) and Hβ(Cys[23])/NH(Ala[25]), Hα-(Ala[30])/NH(Lys[33]), Hα(Arg[29])/Hδ(Asn[17]), Hα(Cys[28])/Hδ-(Asn[17]).

(B) 31–37 Linker Segment. The continuous stretch of NH/NH connectivities present on the NOESY spectra of the native (13–64)NCp7 was not seen for the mutated protein (Figure 1, supplementary material). Moreover, the NH/Hα signals were more intense for the mutated peptide, in agreement with a difference in the conformation of the linker in this peptide. Some cross-correlation peaks, not observed for (13–64)NCp7, were seen with the Cys[23] mutant (Figure 3).

(C) 36–64 C-Terminal Region. The backbone conformation of the distal zinc finger seemed to be almost unaltered by the His[23] to Cys mutation. In contrast, the pattern of NOEs involving residues of this zinc finger and protons of the N-terminal part of the two peptides was clearly different. Figure 4 shows that the NOEs involving the H[4] proton of W[37] and the Hβ protons of Phe[16] found in (13–64)NCp7 as well as in NCp7 (Morellet *et al.*, 1992, 1994) were not observed in Cys[23](13–64)NCp7. The NOEs ββ′(Lys[33])/H_2(Trp[37]) were present in both peptides, but neither the Hγ(Arg[32])/

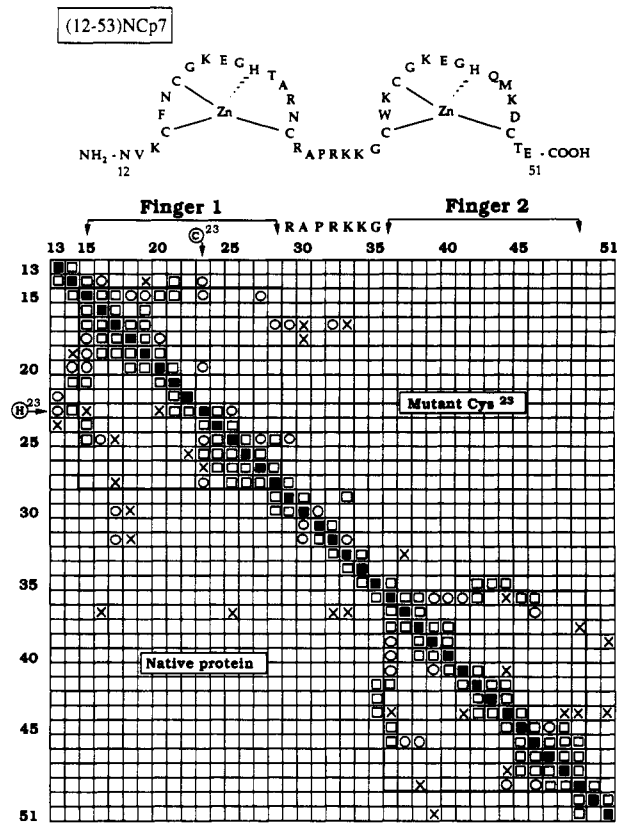

FIGURE 3: Diagonal plot of NOEs for the region V[13]–E[51] of the (upper part) mutant Cys[23](13–64)NCp7 and (lower part) native (13–64)NCp7. Symbols: □, backbone/backbone NOE; ○, backbone/side-chain NOE; ×, side-chain/side-chain NOE.

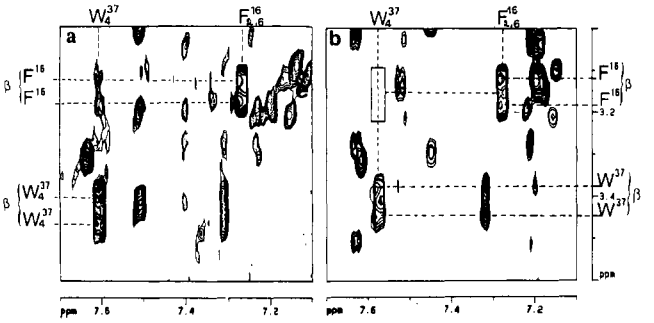

FIGURE 4: Selected regions of the 200-ms NOESY spectra of (a) (13–64)NCp7, pH 6.5 in 90% H_2O/10% D_2O, and (b) Cys[23](13–64)NCp7, pH 6.5 in 90% H_2O/10% D_2O at 20 °C. Comparison of cross peaks shows that the Hβ Phe[16]/H-4 Trp[37] NOE disappears in Cys[23](13–64)NCp7.

H_2(Trp[37]) nor Hγ(Arg[32])/H_7(Trp[37]) cross-correlation peaks were observed in the mutant. Moreover, supplementary NOEs Hβ(Lys[33]), Hγ (Lys[33])/Hε1(Trp[37]) were found in the Cys[23]-(13–64)NCp7. Thus, the replacement of His[23] by Cys[23] abolished the spatial proximity between the two zinc fingers and led to a reorientation of the linker region with respect to the second finger domain. The C-terminal region R[52]–Y[64] of the Cys[23] mutant was found, as was the case in the native protein, to adopt a flexible conformation with a helical element involving the F[56]–G[58] region.

Results of Structure Calculations. A total of 636 relevant distance constraints were used as input for the structure calculations (259 intraresidual and 377 interresidual). Of these, 194 were sequential, 96 medium-range and 87 long-range, constraints. No NH–S or NH–O hydrogen bonds were introduced. The distribution of the distance constraints as a function of the residue index (data not shown) confirms the presence of two folded domains, corresponding to the zinc fingers, joined by a less constrained linker and surrounded by flexible N- and C-terminal regions. For the 50–64 C-terminal sequence, only sequential NOEs were observed, except for the Phe[56]–Gly[58] region. The 20 best structures, generated using DIANA calculations, were further minimized using AMBER as described (Morellet *et al.*, 1992, 1994). The final total energy was 140 ± 12 kcal, which is in the range reported for proteins of similar size (Clore *et al.*, 1987).

Description of the 3D Structure of Cys[23](13–64)NCp7. Good convergence was achieved for Cys[15]–Cys[28] and Cys[36]–Cys[49] domains, with pairwise root mean square deviation values of 0.9 ± 0.4 and 0.9 ± 0.2, respectively. The folding of the mutated zinc finger in Cys[23](13–64)NCp7 was found to be almost identical to that observed for the corresponding mutant CCCC box alone (Jullian *et al.*, 1993). The sequences Arg[29]–Gly[35] and Arg[52]–Tyr[64] did not converge to a unique conformation, in agreement with the absence of long-range NOEs. More detailed information about the similarities and differences between the (13–64)NCp7 peptide and the Cys[23] mutant is given below. The Cys[15]–Cys[18] fragment in the proximal zinc finger forms a type III β turn characterized by the dihedral angle values of Phe[16] (Φ = −65 ± 11°, Ψ = −28 ± 15°) and of Asn[17] (Φ = −58 ± 6°, Ψ = −56 ± 10°). The side-chain amide proton of Asn[17] appears to be hydrogen bonded with the carbonyl oxygen of Gly[29], and the carbonyl oxygen of Cys[15] is pointing in a direction consistent with hydrogen bonding to the NH of Gly[19]. This leads the Hβ and Hγ protons of Lys[14] to be in the vicinity of the Gly[19] Hα protons. The Lys[20]–Cys[23] residues are involved in a type III β-turn conformation with dihedral angle values (Φ = −90 ± 31°, Ψ = −31 ± 93°) for Glu[21] and (Φ = −24 ± 62°, Ψ = −2 ± 72°) for Gly[22]. The Thr[24] carbonyl oxygen allows the formation of a hydrogen bond with the backbone amide protons of Arg[26] and Asn[27]. As shown in Figure 5, the methyl groups of Thr[24] and Ala[25] are not close to the hydrophobic side chain of Phe[16], in contrast to the situation found in NCp7 (Summers *et al.*, 1992; Morellet *et al.*, 1994). Superposition of the computed Cys[15]–Cys[28] backbone on the corresponding backbone structure found in the native protein afforded a RMSD of 2.7 ± 0.7; this value decreased to 1.4 ± 0.1 if only the segment 15–22 was taken into account, in complete agreement with results of a preliminary study on the Cys[23](13–30)NCp7 zinc finger (Jullian *et al.*, 1993). The lower number of observed NOEs involving the Arg[29]–Gly[35] residues in the mutant reflects the greater flexibility of the spacer as compared to that of the wild-type peptide. In agreement with the almost identical chemical shifts and internal NOEs observed in the two peptides, superposition of the Cys[36]–Cys[49] region of Cys[23](13–64)NCp7 and (13–64)NCp7 yielded a mean pairwise RMSD of 1.0 ± 0.1 when only the backbone atoms were taken into account (Figure 2, supplementary material). Attention was paid to the side chain of Trp[37], as it has been proposed that the orientation of this residue in NCp7 could be biologically relevant (Morellet *et al.*, 1993). In the mutant Cys[23](13–64)NCp7, two families of conformers could be distinguished on the basis of the χ_1 dihedral angle of Trp[37]. Fifteen structures had χ_1 values between 17° and 82° and five between −55° and −120°. In the native peptide, all Trp[37] χ_1 values were between 147° and 220°. Thus, the side chain of Trp[37] adopted different orientations and therefore sweeped distinct conformational spaces in the native and mutant peptides (Figure 2, supplementary material). As shown in Figure 6, the flexibility of the linker region of Cys[23](13–64)NCp7 permits the second zinc finger to sweep a larger area of conformational space,

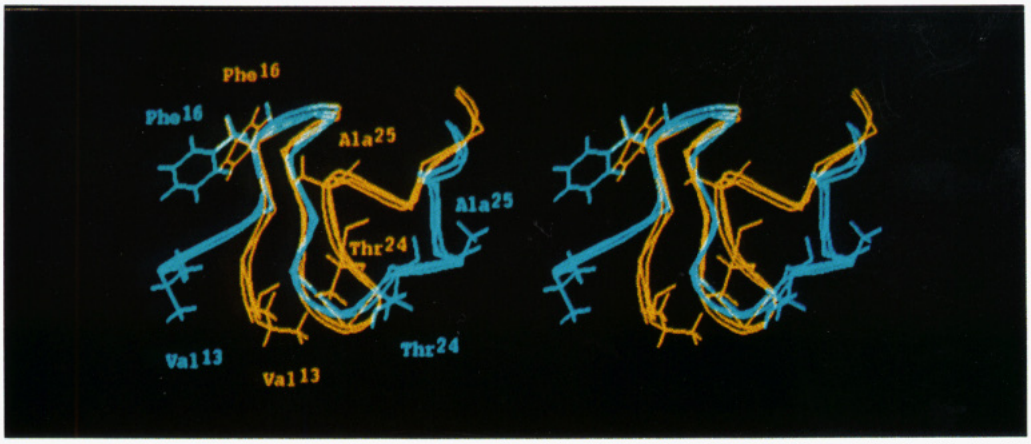

FIGURE 5: Stereoviewed comparison of the 13–30 zinc finger domain of Cys^{23}(13–64)NCp7 (blue) and (13–64)NCp7 (yellow). The side chains of Val^{13}, Phe^{16}, Thr^{24}, and Ala^{25} are represented for both peptides, showing the conformational changes induced by the Cys^{23} mutation. In contrast to the native zinc finger, the Thr^{24} and Ala^{25} in the mutant are not clustered with the other hydrophobic Val^{13} and Phe^{16} side chains.

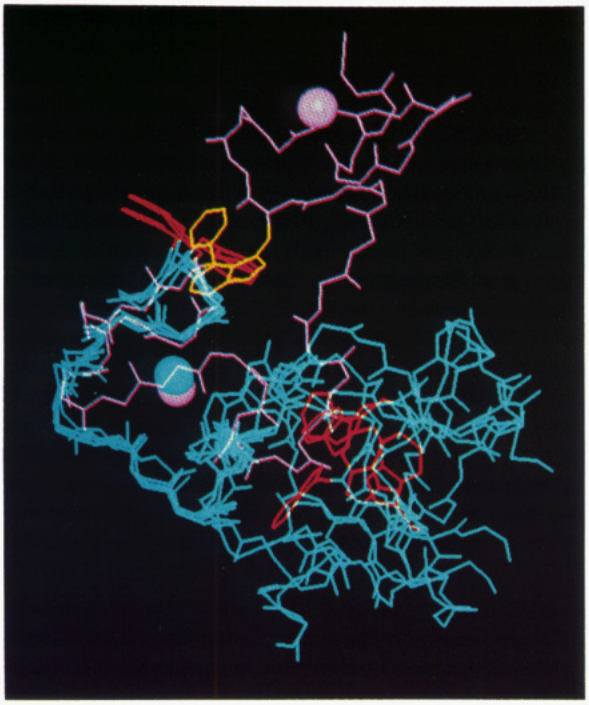

FIGURE 6: Superposition of the first zinc finger of (13–64)NCp7 (purple) upon six conformers of Cys^{23}(13–64)NCp7 (blue). From the Cys^{28} position, the Cys^{23}(13–64)NCp7 conformers sweep a region distinct from that found in the native peptide. Thus in the mutant, the Phe^{16} side chain is maintained away from that of Trp^{37} (residues in yellow). In contrast, in the native (13–64)NCp7, the aromatic rings (residues in red) are in proximity.

but in none of the conformers does it overlap the area occupied by the second zinc finger of the folded structure of (13–64)-NCp7. In the mutant, the mean distance between the aromatic centers of Trp^{37} and Phe^{16} ranged from 9 to 19 Å, while a distance in the 4.8–7.1-Å range was found in NCp7 (Morellet *et al.*, 1994). As expected, a similar result was obtained when the C-terminal zinc fingers of (13–64)NCp7 and its Cys23 mutant were superimposed.

Fluorescence Studies. As the intrinsic fluorescence of (1–55)NCp7 has been shown to be greatly increased in the presence of zinc (Summers *et al.*, 1992), a zinc titration of Cys^{23}(13–64)NCp7 was performed and compared to that of the unmodified (13–64)NCp7 (Figure 3, supplementary material). Since both Trp^{37} and Trp^{61} are in the C-terminal region of the peptides, the fluorescence increase is thought to essentially reflect the binding of zinc to the C-terminal finger. The titration curve of (13–64)NCp7 was nearly linear with a plateau for 2 equiv of zinc, indicating that the binding affinities of both fingers are similar. In contrast, the zinc titration of the C-terminal finger Cys^{23}(13–64)NCp7 was essentially complete at a 1.25:1 zinc to peptide ratio, suggesting that the affinity of the N-terminal CCCC finger for zinc was slightly decreased. Assuming that the C-terminal finger affinity K_2 is about 10^{13} M^{-1} as for the related NCp10 protein (Mély *et al.*, 1991) and that the binding of zinc is not cooperative, we determined that the affinity K_1 of the N-terminal finger was decreased by about 1 order of magnitude (Figure 3, supplementary material). Moreover, the quantum yield of Cys^{23}(13–64)NCp7 in the presence of an excess of zinc ($\Phi = 0.121 \pm 0.007$) was significantly lower than that of (13–64)NCp7 ($\Phi = 0.160 \pm 0.006$), suggesting that the environment of either or both Trp^{37} and Trp^{61} residues is modified. Finally, the accessibility of Trp residues to iodide (an external fluorescence quencher) was found to be significantly larger in Cys^{23}(13–64)NCp7 than in (13–64)NCp7 (data not shown), in agreement with the results of the ^{1}H NMR study.

The Cys^{23}(13–64)NCp7 Mutant Poorly Interacts with HIV-1 RNA and Primer tRNA^{Lys,3} in Vitro. We investigated the consequences of modifying the first zinc finger of the NC protein on the *in vitro* nucleic acid binding and annealing activities of Cys^{23}(13–64)NCp7. The binding of Cys^{23}(13–64)NCp7 to HIV-1 ^{32}P-RNA (positions 1–415) was examined by 5% polyacrylamide gel electrophoresis in the presence of 0.1% SDS (see Experimental Procedures). NCp7 as well as (13–64)NCp7 was able to form stable viral NC protein–RNA complexes under our *in vitro* conditions (see Figure 7, lanes 2–4 and 5–7, respectively). In contrast, Cys^{23}(13–64)NCp7 formed unstable NC protein–RNA complexes only at a high NC protein to viral RNA ratio (Figure 7, lanes 8–10). A basic, but inactive NCp10-derived peptide of MoMuLV was unable to form nucleoprotein complexes (lanes 11 and 12; de Rocquigny *et al.*, 1993).

To confirm that the His^{23} to Cys mutation caused an inhibition of NC protein–RNA interactions, ultraviolet light irradiation at 252 nm was used since it has been shown that UV light links proteins to nucleic acids when reactive groups are no more than 0.1 nm apart (Havron & Sperling, 1977). NCp7 and (13–64)NCp7 stably interacted with replication primer tRNA^{Lys,3} and HIV-1 ^{32}P-RNA since complexes formed of NC protein–RNA at a 1:1 ratio as well as high molecular weight nucleoprotein complexes were observed (Figure 8, lanes 3–5). Cys^{23}(13–64)NCp7, however, was very poorly active since only low levels of NC protein–RNA

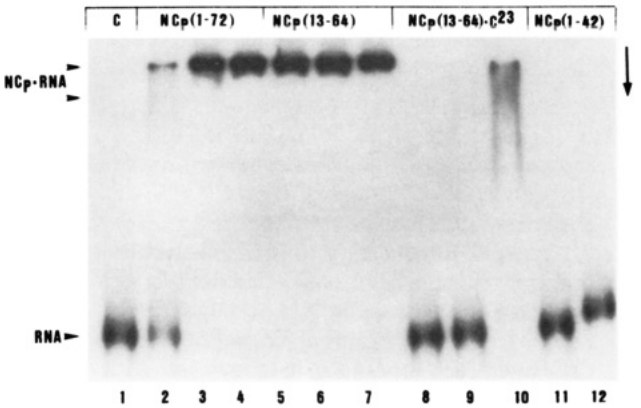

FIGURE 7: Gel retardation assays of viral NC protein–RNA nucleoprotein complexes. Experiments with HIV-1 ^{32}P-RNA of 415 nucleotides and NC protein were carried out as described in Experimental Procedures. The various NC peptides were NCp7 (wild type 1–72) at 0.15, 0.34, and 0.6 μM (lanes 2–4, respectively), (13–64)NCp7 at 0.2, 0.5, and 1 μM (lanes 5–7, respectively), Cys^{23}-(13–64)NCp7 at 0.2, 0.5, and 1 μM (lanes 8–10, respectively), and (1–42)NCp10 of murine leukemia virus as a basic inactive peptide at 1 and 2 μM (lanes 11 and 12, respectively). The ribonucleoprotein complexes are shown (NCp–RNA) as well as free viral RNA. The arrow indicates the direction of electrophoresis. Autoradiography was for 3 h.

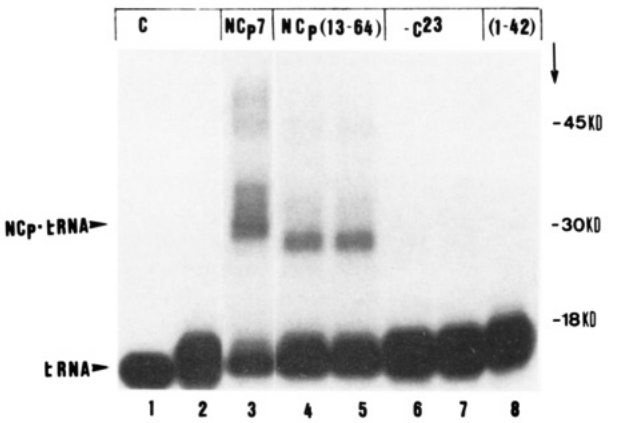

FIGURE 8: UV cross-linking analysis of the interactions of Cys^{23}-(13–64)NCp7 with primer tRNA^{Lys,3}. Lanes: 1, NCp7 at 0.3 μM bound to ^{32}P-tRNA^{Lys,3} without UV irradiation; 2, free tRNA^{Lys,3} UV irradiated for 5 min; 3, NCp7 at 0.2 μM bound to tRNA^{Lys,3} and UV irradiated; 4 and 5, (13–64)NCp7 at 0.1 and 0.3 μM bound to tRNA^{Lys,3} and UV irradiated; 6 and 7, Cys^{23}(13–64)NCp7 at 0.2 and 0.4 μM bound to tRNA^{Lys,3} and UV irradiated; 8, MuLV (1–42)NCp10 at 1 μM bound to tRNA^{Lys,3} and UV irradiated. Samples were processed and analyzed as reported in Experimental Procedures. The 1:1 NC protein–tRNA nucleoprotein complex (NC-tRNA), free tRNA, and molecular mass markers in kilodaltons (kDa) are indicated. The arrow shows the direction of electrophoresis. Autoradiography was for 14 h.

complexes were formed in the presence of primer tRNA^{Lys,3} (Figure 8, lanes 6 and 7; lane 8 corresponded to the inactive NCp10-derived peptide) or HIV-1 ^{32}P-RNA (not shown). As expected, Cys^{23}(13–64)NCp7 did not efficiently promote the annealing of primer tRNA^{Lys,3} onto the primer binding site of the viral RNA (data not shown).

These results clearly show that substitution of Cys for His^{23} in the first zinc finger of HIV-1 nucleocapsid protein resulted in a strong inhibition of the viral RNA binding and annealing activities of the HIV-1 (13–64)NCp7 protein *in vitro*. These observations prompted us to examine the consequences of the His^{23} to Cys mutation on virus production and infectivity.

HIV-1 Virions with a His^{23} to Cys Mutation in NC Are Noninfectious. The importance of the conformation of the first NC zinc finger of HIV-1 was investigated *in vivo* by

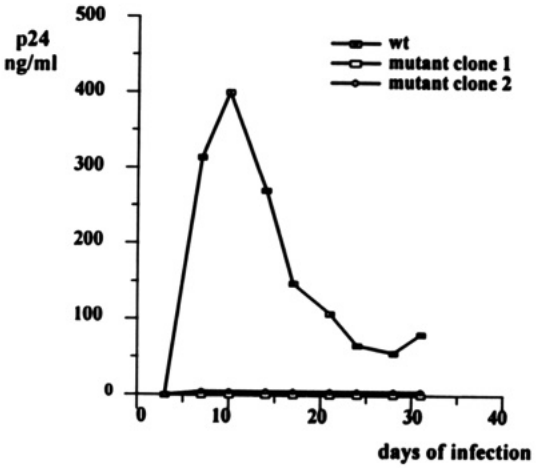

FIGURE 9: Infectivity of the HIV-1 Cys^{23}-NC mutant on human sup T_1 cells showing the absence of infectivity measured by the amount of CAp24 in the medium.

substituting Cys for His^{23} in two infectious HIV-1 molecular clones using site-directed mutagenesis (HIV-1 LAI and pNL4.3; see Experimental Procedures). Wild-type HIV-1 DNA and Cys^{23}-NC DNA were introduced into Cos7 cells by transfection, and the virions produced were analyzed for their protein and RNA content and their infectivity.

Equivalent levels of wild-type and Cys^{23} HIV-1 virions were produced by cells transfected with wild-type and Cys^{23}-NC DNA, as determined by CAp24 ELISA and reverse transcriptase (RT) activity (see Experimental Procedures). Virus infectivity was examined upon infection of human SupT1 cells and subsequent formation of syncitia and release of virion-associated RT activity. The HIV-1 Cys^{23}-NC mutant was not infectious 3 weeks after cell infection (Figure 9), while the infectious titer of the wild-type virus was 10^6 infectious particles per 10 ng of CAp24 when measured by the end-point dilution procedure.

The protein content of HIV-1 Cys^{23}-NC virions was examined by SDS–PAGE and immunoblotting (see Experimental Procedures). Mature GAG proteins as well as some Pr55gag precursor were found to constitute the major core proteins of both the wild-type and Cys^{23}-NC virions.

HIV-1 viral RNA from the Cys^{23}-NC mutant and wild-type virions was analyzed by northern blot (see Experimental Procedures) and the unspliced genomic RNA detected using a ^{32}P-DNA probe corresponding to the gag and pol sequences. The content of genomic RNA in Cys^{23}-NC mutant virions was reduced to about 15% of the wild-type level (Figure 10; compare lanes 1 and 3). The virion genomic RNA of HIV-1 and other retroviruses is known to be susceptible to nuclease degradation [see Coffin (1984) and Darlix *et al.* (1991)], and only a fraction of genomic RNA was full length in wild-type virions (lane 3). Interestingly, the genomic RNA present in Cys^{23}-NC mutant virions was extensively degraded and no full-length genomic RNA could be observed (lane 1).

DISCUSSION

Various types of zinc binding domains, differing by the ratio of cysteine/histidine residues and by the number of amino acids present between the metal binding ligands, have been found in proteins that have been implicated in nucleic acid recognition (Berg *et al.*, 1990; Angrand, 1993). In the case of retroviruses, a zinc finger domain of the $CX_2CX_4HX_4C$ form is highly conserved. The aim of the present study was to investigate the structural role played by this metal binding domain in the various functions of the HIV-1 NCp7. For this

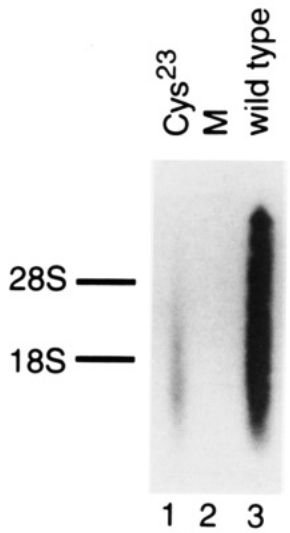

FIGURE 10: Northern blot analysis of the genomic RNA present in the Cys[23]-NC mutant virions. Virions were collected and the genomic RNA was purified as described in Experimental Procedures. Northern blot analysis was performed according to a published procedure. The unspliced genomic RNA was detected by means of hybridizing a ^{32}P-labeled probe corresponding to the gag and pol sequences of HIV-1. 18S and 28S indicate the position of ribosomal 18S and 28S tRNA of 2000 and 5000 nt, respectively. M is mack infection. Electrophoresis was from top to bottom. Autoradiography was for 24 h.

purpose, the histidine residue in the first zinc finger was replaced by Cys and the solution structure of the mutant Cys[23]-(13–64)NCp7 studied by 2D ^{1}H NMR spectroscopy. In a preliminary study we showed that the replacement of His[23] by Cys in the proximal zinc finger of NCp7 in the (13–30)-NCp7 peptide did not preclude the binding of Zn^{2+} but did produce a change in its structure, resulting in a drastic modification of the spatial orientation of numerous side chains (Phe[16], Thr[24], Ala[25]) and of the short Cys[23]–Cys[28] domain preceding the linker region (Jullian *et al.*, 1993). This was interpreted to result from a spatial rearrangement of the peptide backbone to allow tetrahedral coordination of the zinc ion by the four cysteines (Jullian *et al.*, 1993). The present study shows that the introduction of the His[23] to Cys mutation in the active (13–64)NCp7 did not significantly alter its affinity for the zinc ion as shown by fluorescence studies. In addition, while the folding of the C-terminal zinc finger was not affected by the His[23] to Cys change, large structural modifications of the entire Cys[23](13–64)NCp7 peptide were observed. Thus, in addition to a conformational change in the proximal finger, similar to that already observed in the N-terminal finger alone, the mutation induced a modification in the spatial orientation of the short linker region with a subsequent increase in the distance between both zinc fingers. Indeed, the distance between the aromatic ring centers of Phe[16] and Trp[37], as evaluated by fluorescence, increased from 4.8–7.1 Å in the native protein (Morellet *et al.*, 1992, 1994) to between 9 and 18 Å in the Cys[23] mutant. This is in agreement with the disappearance of the NOE effects between Phe[16] and Trp[37] and more generally between the protons of the linker and the zinc finger domains (Figures 3 and 4). The small or medium NOEs accounting for the spatial proximity between the two zinc fingers of NCp7 were not observed in other studies (Omichinski *et al.*, 1991; South & Summers, 1993). This could be due to differences in the conditions of NMR studies (concentration of NCp7, pH, temperature, *etc.*) as recently discussed in detail (Morellet *et al.*, 1994). Nevertheless, the biological relevance of the internally folded structure of NCp7 is supported by an increase in the intensities of several interfinger NOEs occurring in the complex between NCp7 and a single-stranded oligonucleotide belonging to the HIV genome (Déméné *et al.*, manuscript in preparation).

Fluorescence experiments confirmed that the replacement of His[23] by Cys in Cys[23](13–64)NCp7 led to an increase in the Trp accessibility to iodine as compared to the wild-type NCp7 (Mély *et al.*, 1994). In a recent NMR study, South and Summers (1993) have shown that the pentadeoxynucleotide ACGCC corresponding to a ribonucleotide sequence found in the genomic RNA packaging domain (Aldovini & Young, 1990) interacts with the N-terminal finger of NCp7 (MN strain). The side chains of Val[13], Phe[16], Ile[24] (Thr[24] in our case), and Ala[25] were shown to be involved in the complex which appeared stabilized both by an electrostatic interaction between the positively charged Arg[26] side chain and a nucleic acid phosphodiester group and by an hydrogen bond involving the carboxyl oxygen of Lys[14] and the guanosine N1H atom (South & Summers, 1993). Interestingly, residues Trp[37], Lys[38], Gln[45], and Met[46], which lie on the same side of the molecule as Val[13], Lys[14], Phe[16], Thr[24], and Ala[25] in the folded structure of (13–64)NCp7 (this study) and NCp7 (Morellet *et al.*, 1994) and which are thus good candidates for interactions with target nucleic acids, are scattered in the mutant Cys[23](13–64)NCp7 in all DIANA conformers (Figure 6). Moreover, the replacement of His[23] by Cys in Cys[23]-(13–64)NCp7 induced a change in the spatial orientation of the Cys[23]–Cys[28] segment, thus increasing the size of the hydrophobic cleft formed by the Val[13], Phe[16], Thr[24], and Ala[25] side chains (South & Summers, 1993; Morellet *et al.*, 1994) (Figure 5).

These structural changes prevent efficient nucleic acid recognition as shown *in vitro* by a low level of viral RNA binding as measured by gel mobility and UV cross-linking assays (Figure 7). The drastic reduction in RNA binding affinity of Cys[23](13–64)NCp7 resulted in the *in vitro* inability of this peptide to promote the annealing of replication primer ^{32}P-tRNA^{Lys,3} to the primer binding site of the HIV-1 RNA (Figure 8) and to promote dimerization of the 1–415 HIV-1 genomic segment that contains the packaging–dimerization signal (not shown). *In vitro* experiments have indicated that the zinc fingers of NCp7 are not directly required for RNA dimerization and annealing of the primer tRNA^{Lys,3} to the PBS. However, the V[13]K, R[30]APRKK[34], and T[50]ERQAN-FLGKIWPSY[64] sequences, which correspond to the basic domains flanking the metal binding motifs, have been specifically implicated in the RNA annealing activities of NCp7 (de Rocquigny *et al.*, 1992). The low RNA binding affinity observed *in vitro* with Cys[23](13–64)NCp7 suggests that the overall structural change observed by ^{1}H NMR prevents at least one of the basic regions from interacting with its nucleic acid target. *In vivo*, Cos cells transfected with HIV-1 DNA containing the His[23] to Cys mutation generated normal levels of viral particles. However, these viral particles were completely noninfectious, even though they contained mature proteins indicating that the gag and gag–pol polyproteins had been packaged and processed into the virions. In addition, a comparative northern blot analysis showed that, despite a drastic reduction in binding to RNA *in vitro*, the Cys[23] mutant viruses presented only a 6-fold reduction in genomic RNA levels. This result supports the notion that the N- and C-terminal domains of NCp7, either in the free protein or as part of the gag polyprotein precursor, participate in genomic RNA packaging or that domains of the gag polyprotein, outside the NCp7 sequence, should be able to encapsidate small amounts of the viral RNA (Oertle & Spahr,

1990; Aronoff *et al.*, 1993; Berkowitz *et al.*, 1993). It is interesting to note that the impairment of genomic RNA encapsidation observed with this HIV-1 NC mutant is similar to that seen with the mutant in which the proximal zinc finger was mutated so as to hinder tetrahedral coordination of the metal and subsequent folding of the CCHC motif (Aldovini & Young, 1990; Gorelick *et al.*, 1990; Dorfman *et al.*, 1993).

As there is no absolute correlation between the level of virion infectivity and the amounts of encapsidated RNA [see also Dorfman *et al.* (1993)], the lack of virus infectivity of the Cys^{23} mutant could be due to additional factors. NC protein has been shown to be important for the protection of genomic RNA from nuclease degradation in avian retroviruses (Aronoff *et al.*, 1993). Therefore, the loss of infectivity of the Cys^{23} mutant might be due, at least in part, to the inability of Cys^{23}(NCp7) to protect the genomic RNA from nuclease digestion. This is supported by the absence of full-length RNA in the viral particles produced by the mutant and by the strong reduction in RNA binding of Cys^{23}(13–64)NCp7 *in vitro*.

It is interesting to notice that another type of mutation, i.e., the replacement by D-Pro or Leu for the Pro^{31} residue located in the short spacer linking the two zinc fingers, did not modify the folding of these domains but induced a change in their mutual orientation. This was shown to result in a 2-fold reduction in RNA annealing activities *in vitro*. *In vivo*, the Leu^{31} mutation led to noninfectious virions which contained normal levels of viral RNA but no gag–pol precursor (Morellet *et al.*, 1994). Taken together, all these findings show that the integrity of the two zinc fingers is essential for efficient RNA recognition *in vivo* but that the nature of the linker and probably its role in directing the conformation of NCp7 is critical for encapsidation of gag–pol precursor into virions. All these results could be taken into account for the rational design of compounds aimed at blocking one of the functions of NCp7.

ACKNOWLEDGMENT

We thank R. Ruffault for her efficient technical assistance. We are grateful to Miss C. Dupuis for expert manuscript drafting and M. Lapadat and J. Vierek for critical revision of the manuscript.

SUPPLEMENTARY MATERIAL AVAILABLE

A table of the chemical shifts of the Cys^{23}(13–64)NCp7 and (13–64)NCp7 peptides at pH = 6.5, T = 20 °C, a summary of the short- and medium-range NOEs involving NH, αH, and βH protons observed for the Cys^{23}(13–64)NCp7 and (13–64)NCp7 peptides, a figure representing a stereoview of the 36–49 domains of the Cys^{23}(13–64)NCp7 and (13–64)NCp7 peptides, and the zinc titration of the fluorescence of the Cys^{23}-(13–64)NCp7 and (13–64)NCp7 peptides (7 pages). Ordering information is given on any current masthead page.

REFERENCES

Adachi, A., Gendelman, H. E., Koenig, S., Folks, T., Wiley, R., Rabson, A., & Martin, M. A. (1986) *J. Virol. 59*, 284–291.

Aldovini, A., & Young, R. A. (1990) *J. Virol. 64*, 1920–1926.

Angrand, P. O. (1993) *Med. Sci. 9*, 725–736.

Aronoff, R., Hajjar, A. M., & Linial, M. L. (1993) *J. Virol. 67*, 178–188.

Arseniev, A., Schultze, P., Wörgötter, T., Braun, W., Wagner, G., Vasak, M., Kägi, J. H. R., & Wüthrich, K. (1988) *J. Mol. Biol. 201*, 637–657.

Barat, C., Lullien, V., Schatz, O., Keith, G., Nugeyre, M. T., Gruninger-Leitch, F., & Barre-Sinoussi, F. (1989) *EMBO J. 8*, 3279–3285.

Barat, C., Le Grice, S. F. J., & Darlix, J. L. (1991) *Nucleic Acids Res. 19*, 751–757.

Berg, J. M. (1986) *Science 232*, 485–487.

Berg, J. M. (1990) *J. Biol. Chem. 265*, 6513–6516.

Berkowitz, R. D., Luban, J., & Goff, S. P. (1993) *J. Virol. 67*, 7190–7200.

Bieth, E., Gabus, C., & Darlix, J. L. (1990) *Nucleic Acids Res. 18*, 119–127.

Braunschweiler, L., & Ernst, R. R. (1983) *J. Magn. Reson. 43*, 259–291.

Chen, C., & Okayama, H. (1987) *Mol. Cell. Biol. 7*, 2745–2752.

Clore, G. M., Sukumaran, D. K., Nilges, M., Zarbock, J., & Cronenborg, A. M. (1987) *EMBO J. 6*, 529–537.

Coffin, J. M. (1984) in *RNA Tumor Viruses* (Weiss, R., Teich, N., Varmus, H., & Coffin, J. M., Eds.) Vol. 1, pp 261–368, Cold Spring Harbor Laboratory Press, Cold Spring Harbor, NY.

Darlix, J. L. (1991) *Bull. Inst. Pasteur 89*, 211–242.

Darlix, J. L., Gabus, C., Nugeyre, M. T., Clavel, F., & Barré-Sinoussi, F. (1990) *J. Mol. Biol. 216*, 689–699.

Davis, D. G., & Bax, A. (1985) *J. Am. Chem. Soc. 107*, 2821–2822.

Déméné, H., Jullian, N., Morellet, N., de Rocquigny, H., Cornille, F., Maigret, B., & Roques, B. P. (1994) *J. Biomol. NMR 4*, 153–170.

de Rocquigny, H., Ficheux, D., Gabus, C., Fournié-Zaluski, M. C., Darlix, J. L., & Roques, B. P. (1991) *Biochem. Biophys. Res. Commun. 180*, 1010–1018.

de Rocquigny, H., Gabus, C., Vincent, A., Fournié-Zaluski, M. C., Roques, B. P., & Darlix, J. L. (1992) *Proc. Natl. Acad. Sci. U.S.A. 89*, 6472–6476.

de Rocquigny, H., Ficheux, D., Gabus, C., Fournié-Zaluski, M. C., Darlix, J. L., & Roques, B. P. (1993) *Nucleic Acids Res. 21*, 823–829.

Dorfman, T., Luban, J., Goff, S. P., Haseltine, W. A., & Göttlinger, H. G. (1993) *J. Virol. 67*, 6159–6169.

Dupraz, P., Oertle, S., Méric, C., Damay, P., & Spahr, P. F. (1990) *J. Virol. 64*, 4978–4987.

Eisinger, J., & Navon, G. (1969) *J. Chem. Phys. 50*, 2069–2077.

Fitzgerald, D. W., & Coleman, J. E. (1991) *Biochemistry 30*, 5195–5200.

Goff, S., Traktman, P., & Baltimore, D. (1981) *J. Virol. 38*, 239–248.

Gorelick, R. J., Henderson, L. E., Hanser, J. P., & Rein, A. (1988) *Proc. Natl. Acad. Sci. U.S.A. 85*, 8420–8424.

Gorelick, R. J., Nigida, S. M., Jr., Bess, J. W., Jr., Arthur, L. O., Henderson, L. E., & Rein, A. (1990) *J. Virol. 64*, 3207–3211.

Göttlinger, H. G., Sodroski, J. G., & Haseltine, W. A. (1989) *Proc. Natl. Acad. Sci. U.S.A. 86*, 5781–5785.

Green, L. M., & Berg, J. M. (1990) *Proc. Natl. Acad. Sci. U.S.A. 86*, 4047–4051.

Griesinger, C., Otting, G., Wüthrich, K., & Ernst, R. R. (1988) *J. Am. Chem. Soc. 110*, 7870–7872.

Güntert, P., Braun, W., & Wütrich, K. (1991a) *J. Mol. Biol. 217*, 517–530.

Güntert, P., Qian, Y. Q., Offing, O., Müller, M., Gehring, W., & Wüthrich, K. (1991b) *J. Mol. Biol. 217*, 531–540.

Havron, A., & Sperling, J. (1977) *Biochemistry 16*, 5631–5635.

Henderson, L. E., Copeland, T. D., Sowder, R. C., Smythers, G. W., & Orozland, S. (1981) *J. Biol. Chem. 256*, 8400–8406.

Jacob, O. (1990) Ph.D. Thesis, Université Louis Pasteur, Strasbourg, France.

Jeener, J., Meier, B. H., Bachmann, P., & Ernst, R. R. (1979) *J. Chem. Phys. 71*, 4546–4553.

Jullian, N., Déméné, H., Morellet, N., Maigret, B., & Roques, B. P. (1993) *FEBS Lett. 331*, 43–48.

Kochoyan, M., Havel, T. F., Nguyen, D. T., Dahl, C. E., Keutmann, H. T., & Weiss, M. A. (1991) *Biochemistry 30*, 3371–3886.
Kunkel, T. A. (1985) *Proc. Natl. Acad. Sci. U.S.A. 82*, 488–492.
Macurra, S., Huang, Y., Suter, D., & Ernst, R. R. (1981) *J. Magn. Reson. 43*, 259–281.
Marion, D., & Wüthrich, K. (1983) *Biochem. Biophys. Res. Commun. 113*, 967–974.
Mély, Y., Cornille, F., Fournié-Zaluski, M. C., Darlix, J. L., Roques, B. P., & Gérard, D. (1991) *Biopolymers 31*, 899–906.
Mély, Y., Jullian, N., Morellet, N., de Rocquigny, H., Fournié-Zaluski, M. C., Roques, B. P., & Gérard, D. (1994) *Biochemistry* (in press).
Méric, C., & Goff, S. P. (1989) *J. Virol. 63*, 1558–1568.
Méric, C., Gouilloud, E., & Spahr, P. F. (1988) *J. Virol. 62*, 3328–3333.
Morellet, N., Jullian, N., de Rocquigny, H., Maigret, B., Darlix, J. L., & Roques, B. P. (1992) *EMBO J. 11*, 3059–3065.
Morellet, N., de Rocquigny, H., Mély, Y., Jullian, N., Déméné, H., Ottmann, M., Gérard, D., Darlix, J. L., Fournié-Zaluski, M. C., & Roques, B. P. (1994) *J. Mol. Biol. 235*, 287–301.
Oertle, S., & Spahr, P. F. (1990) *J. Virol. 64*, 5757–5763.
Omichinski, J. G., Clore, G. M., Sakaguchi, K., Appella, E., & Cronenberg, A. M. (1991) *FEBS Lett. 292*, 25–30.
Pearlman, D. A., Case, D. A., Caldwell, J. C., Seibel, G. L., Singh, U. C., Weiner, P., & Kollman, P. A. (1991) *Amber 4.0*, University of California, San Francisco.
Peden, K., Emerman, M., & Montagnier, L. (1991) *Virology 185* (2), 661–672.
Rance, M., Srensen, O. W., Bodenhausen, G., Wagner, G., Ernst, R. R., & Wüthrich, K. (1983) *Biochem. Biophys. Res. Commun. 117*, 479–485.
Schägger, H., & von Jagow, G. (1987) *Anal. Biochem. 166*, 368–379.
Smith, S. D., Shatsky, M., Cohen, P. S., Warnke, R., Lurk, M. P., & Olader, B. (1984) *Cancer Res. 44*, 5657–5660.
South, T. L., & Summers, M. F. (1993) *Protein Sci. 2*, 3–19.
South, T. L., Kim, B., & Summers, M. F. (1989) *J. Am. Chem. Soc. 111*, 395–396.
South, T. L., Blake, P. R., Hare, D. R., & Summers, M. F. (1991) *Biochemistry 30*, 6342–6349.
Summers, M. F., South, T. L., Kim, B., & Hare, D. R. (1990) *Biochemistry 29*, 329–340.
Summers, M. F., Henderson, L. E., Chance, M. R., Bess, J. W., South, T. L., Blake, P. R., Sagi, I., Perez-Alvarado, G., Sowder, R. C., II, Hare, D. R., & Arthur, L. O. (1992) *Protein Sci. 1*, 563–574.
Wüthrich, K. (1986) in *NMR of Proteins and Nucleic Acids*, Wiley & Sons, New York.